TOMOGRAPHIC RECONSTRUCTION OF THE LOCAL PDFS OF SOOT VOLUME FRACTION AND TEMPERATURE

Y. R. Sivathanu

School of Mechanical Engineering, Purdue University, W. Lafayette, IN 47906

A. Hamins, C. Hagwood and T. Kashiwagi
The National Institute of Standards and Technology
Gaithersburg, MD 20899

Introduction- Deconvolution of local properties from line-of-sight measurements is important in a wide variety of applications such as x-ray tomography, nuclear magnetic resonance imaging, atmospheric sciences, optical inteferometry and flow field diagnostics. The Radon Transforms[1] form the theoretical basis for retrieving local properties from path integrated measurements under steady state conditions. These methods have found wide-spread application in tomographic spectroscopy of laminar flames[2,3].

For turbulent flow fields, conventional deconvolution algorithms cause greater difficulty due to the transient nature of the phenomena being studied. Progress has been made in obtaining ultra-fast multiple angle and multiple ray measurements in a turbulent flow field over a small time interval[4,5]. This technique has limited temporal resolution and suffers from a high degree of deconvolution noise due to the asymmetric nature of the instantaneous flow field. Recently, a discrete probability function (DPF) method was developed to deconvolute path integrated measurements in order to obtain the local PDFs of soot volume fractions in turbulent flames[6].

The objective of this work is to extend the DPF method to obtain local PDFs of soot volume fraction and temperature from path integrated measurements of emission intensities. The deconvolution method is evaluated by synthetic noise-free data as well as experimental data obtained using an intrusive optical pyrometer.

Experimental apparatus- The optical pyrometer used for obtaining the path integrated intensity measurements is discussed in Ref. 9. In the present work, path integrated measurements of radiation intensity were obtained at 900 nm and 1000 nm from several parallel projections at one angle in an ethylene air flame. The ethylene/air diffusion flame was stabilized on a 4.4 mm burner in a vertical configuration with an exit Reynolds number of 10000. The measurements were obtained 3 mm apart, at an axial height of 220 mm (x/d=50), perpendicular to the flame axis. A horizontal slice of the flame through which measurements at several equally spaced projections were performed is shown in Fig. 1.

The intensity emitted from the parallel projections in the flame was collimated using a 3 mm o.d. stainless steel tube. The collimating tube was painted black on the inside to minimize internal reflections and had a length of 500 mm providing an acceptance view angle of less than half a degree. The intensities were measured using photo-diodes having narrow band optical filters, with half bandwidth of 10 nm, in front of each. The optical pyrometers were calibrated using a standard black body at 1000 °C. The emission intensities were sampled at 1000 Hz per channel for 100 seconds, after adequate signal conditioning. This large number of data points was necessary to obtain relatively noise free (with an RMS error norm of less than 5% for two measurements at the same location) joint PDFs of emission intensities. The optical pyrometer was also used to provide local measurements with a probe separation distance of 5 mm[9].

Numerical method for deconvolution- Consider a horizontal chord through the flame as shown in Figure 1 consisting of M homogeneous segments. The spectral emission intensity, I_λ leaving any segment 'm', is the sum of the incident energy attenuated by the transmittance of the segment, τ_λ and the emission intensity, $I_{\lambda e}$ of the segment and can be expressed as[7]:

$$I_\lambda(m)=I_\lambda(m-1)\tau_\lambda(m)+I_{\lambda e}(m); \quad m=1,...,M \qquad (1)$$

where λ is the wavelength. The transmittance and emission intensity of the segment are related to the soot volume fraction and temperature as follows:

$$\tau_\lambda(m)=\exp(-K_\lambda f_v \Delta s(m)/\lambda) \qquad (2)$$

and
$$I_{\lambda e}=(1.-\exp(-K_\lambda f_v \Delta s(m)))(C_1/\exp(C_2/\lambda T)) \qquad (3)$$

where f_v is the soot volume fraction, T is the temperature, Δs is the length of segment m, K_λ is a constant which depends on the refractive indices of soot[8] and C_1 and C_2 are the radiation constants.

In a turbulent medium, the deconvolution problem is complicated by the fact that the soot volume fraction and temperature fluctuate as a function of time. The instantaneous temperatures and soot volume fractions have large asymmetric local variations at any position in the horizontal plane. However, for the present geometry of fuel exiting a round tube, the PDFs (which are time averaged quantities) are expected to be axi-symmetric. Thus, an onion-peeling deconvolution algorithm can be effectively used to obtain the PDFs of soot volume fraction and temperature from the measured intensities.

The joint DPF of soot volume fraction and temperature can be expressed as[7]:

$$P(T,f_v) \equiv \{(T_i, f_{vj}); P_{Tij}\} : i=1,...,N: j=1,...,N \qquad (4)$$

T_i and f_{vj} are the bin values and P_{Tij} is the probability that T is between T_{i-1} and T_{i+1} while the soot volume fraction is between f_{vj-1} and f_{vj+1}. The joint DPF of soot volume fraction and temperature can be obtained by integrating the joint PDF of soot volume fraction and temperature $g(T,f_v)$ over a small temperature and soot volume fraction range[7]. Similarly, the joint DPF of intensity at two wavelengths, I_λ and I_μ can be obtained from the joint PDF of intensities $g(I_\lambda,I_\mu)$, and can be expressed as:

$$P(I_\lambda,I_\mu) \equiv \{(I_{\lambda k},I_{\mu n}); P_{Ikn}\} : k=1,...,N: n=1,...,N \qquad (5)$$

where P_{Ikn} is the probability that I_λ is between $I_{\lambda k-1}$ and $I_{\lambda k+1}$, whereas I_μ is between $I_{\mu n-1}$ and $I_{\mu n+1}$. For any segment m, the joint DPF of intensity leaving that segment is:

$$P(I_\lambda,I_\mu(m))=P(I_\lambda,I_\mu(m-1))\otimes P(T,f_v(m)) \qquad (6)$$

where $\otimes$ represent a joint convolution-composition operation. This convolution-composition operation can be calculated using the DPF method as follows:

$$P_{Ikn}^m = \sum_k^N \sum_n^N \sum_i^N \sum_j^N P_{Ikn}^{m-1} P_{Tij}^m \, \delta^m(kn) \qquad (7)$$

where $\delta^m(kn)=1$ if $I_{\lambda k-1} < I^m_\lambda < I_{\lambda k+1}$ and $I_{\mu n-1} < I^m_\mu < I_{\mu n+1}$ else $\delta^m(kn)=0$. The superscript m represents the segment number and I^m_λ and I^m_μ are calculated using Eqs. (1-3).

The forward convolution-composition operation represented by Eq. (7) was used to synthetically create the joint PDFs $g(I_\lambda,I_\mu)$ using known joint PDFs of soot volume fraction and

93

temperature $g(T,f_v)$ for an axi-symmetric flame consisting of eight rings. These joint PDFs, were used in the deconvolution algorithm to check the methodology independent of measurement noise and spatial correlation effects.

The deconvolution procedure essentially uses an iterative algorithm. Consider two segments, 1 and 2 with known joint PDFs of intensities $g^1(I_\lambda,I_\mu)$ and $g^2(I_\lambda,I_\mu)$. It is required to find the joint PDF, $g^2(T,f_v)$ from the joint PDFs of intensities. The iterative algorithm starts with a guessed joint PDF $g_n^2(T,f_v)$, uniform in the range of temperatures, 250K to 3000K and soot volume fractions 0 ppm to 30 ppm. These values are used since they represent the highest and lowest possible values of both soot volume fraction and temperatures in ethylene/air diffusion flames. The subscript n indicates the iteration index for the solution of $g^2(T,f_v)$. Eq. (7) is used with $g_n^2(T,f_v)$ and $g^1(I_\lambda,I_\mu)$ to calculate $g_n^2(I_\lambda,I_\mu)$, and is used to find $g_{n+1}^2(T,f_v)$ as:

$$g_{n+1}^2(T,f_v) = \iint g^2(I_\lambda,I_\mu)g_n^2(T,f_v|I_\lambda,I_\mu)\ dI_\lambda dI_\mu \tag{8}$$

where $g_n^2(T,f_v|I_\lambda,I_\mu)$ is the conditional joint PDF of T and fv conditioned on the values of I_λ and I_μ. The conditional PDFs are calculated by using Eq. (7) while keeping track of the indices i and j for the solution of $P(I_\lambda,I_\mu)$. The iteration algorithm converges very fast to the solution $g^2(T,f_v)$. The iteration is terminated (usually in 20 iterations) when the L_2 norm, ε defined as:

$$\varepsilon = \sqrt{\iint (g^2(I_\lambda,I_\mu) - g_n^2(I_\lambda,I_\mu))^2\ dI_\lambda dI_\mu} \tag{9}$$

is less than 0.05.

The joint PDF of the local soot volume fraction and temperature can be obtained only after reducing the path integrated measurements to equivalent two segment problems. An onion-peeling procedure is used to reduce the path integrated measurements into equivalent two segment problems. The deconvolution is started from the outermost ring and the joint PDF of soot and temperature $g^1(T,f_v)$ for the outermost ring is obtained first. This PDF is used with Eq. (7) to obtain $g^1(I_\lambda,I_\mu)$ and $g^3(I_\lambda,I_\mu)$ for the first and third segments of the second ring which consists of three segments, 1, 2 and 3 as shown in Fig. 1. The intensity measured at the second ring, is the sum of the transmitted part of the intensity from the second segment and the emission intensity of segment 3, as outlined in Eq. (1). $g^3(I_\lambda,I_\mu)$ and the measured joint PDF of intensities for the second ring $g^T(I_\lambda,I_\mu)$ is used in an iterative algorithm to obtain $g^2(I_\lambda,I_\mu)$ as follows:

$$g_{n+1}^2(I_\lambda,I_\mu) = \iint g^T(I_\lambda,I_\mu)g_n^2(I_\lambda,I_\mu|I^T{}_\lambda,I^T{}_\mu)\ dI_\lambda dI_\mu \tag{10}$$

where $g^T{}_n(I_\lambda,I_\mu)$ is obtained from the forward convolution of guessed values of $g^2{}_n(I_\lambda,I_\mu)$ and $g^3(I_\lambda,I_\mu)$ utilizing Eqs. (6-7). The superscripts T on the I in Eq. (10) is to differentiate the two joint density functions, one obtained from two segments and the other from three. Having obtained $g^2(I_\lambda,I_\mu)$ and $g^1(I_\lambda,I_\mu)$, the iterative algorithm given by Eq. (8) is used to find the $g(T,f_v)$ for the second segment in the ring.

For the third ring with five segments, forward convolutions are performed on the first two and the last two segments, to reduce the problem to a three-segment problem and solved iteratively using Eqs. (8,10). This 'onion-peeling' technique, is carried forward until the joint density functions of soot and temperature for all the rings in the flame are known.

Numerical and experimental results- The results obtained from the deconvolution of the synthetic data will be discussed first. The advantage of using synthetically created data for the deconvolution algorithm is that the entire method can be checked independently of experimental noise and spatial correlation effects. The mean and RMS values of soot volume fraction and temperature obtained from the deconvolution algorithm, as well as the values used to created the synthetic data are shown in Fig. 2. The results show that the deconvolution algorithm is capable of providing the first two moments of soot volume fraction and temperature if the data is noise free. The deconvolution algorithm can retrieve the PDFs of temperature and soot volume fraction as shown in Fig. 3, for a representative location half way to the edge of the flame.

The deconvolution algorithm is next applied to the path integrated data obtained from the ethylene/air flame. The mean and RMS values of temperature as well as soot volume fraction obtained from the deconvolution algorithm, and their comparison with values obtained using an intrusive probe are shown in Fig. 4. The data from the intrusive probe is much more intermittent than those obtained from the deconvolution, because the shorter flame measurement distance used by the intrusive probe results in a larger fraction of intensity measurements below the detection threshold of the detectors. Therefore, for meaningful comparisons, the probe data for the intermittent signals were neglected, and results are presented only till r=25 mm, while the flame edge extended up to 36 mm. The intrusive data for points above 25 mm have less than 10% of the values yielding detectable signals, and for radiation calculations should not affect the results. There are substantial differences in the data obtained using the two different methods. In particular, the mean and the RMS of soot volume fractions measured by the probe is consistently higher than that obtained from deconvoluting the path integrated measurements. In addition, the RMS of temperature from the probe data is less than that obtained from the deconvolutions. The cross-correlation between soot volume fraction and temperature is around -0.6 for both methods. The differences obtained by the two measurement techniques can be explained by examining the PDFs of soot volume fraction and temperature.

The PDFs of temperature and soot volume fraction are shown in Fig. 5 and Fig. 6 for two different locations along the radius of the flame. The intrusive probe has a finite window of data acceptance. If either the soot volume fraction or the temperature falls outside values from which meaningful intensity signals results, the data are rejected. Consequently, the measurement limit for temperature is approximately 1100 K (as observed previously[9]). Moreover, soot volume fractions and temperatures are negatively correlated, therefore at very high temperatures, we have low soot volume fractions, and the intensity again falls below the detection limit of the intrusive probe. Therefore, we have absence of high temperatures and a smaller amount of low soot volume fractions detected by the intrusive probe.

Conclusion- A tomographic method to obtain the local PDFs of soot volume fraction and temperature in luminous turbulent diffusion flames is presented and validated with experimental data obtained using an intrusive probe. Differences between the two methods could be attributed to the lower detection capabilities of the intrusive probes.

References

1) S. R. Deans, The Radon Transform and some of its Applications, Wiley, New York (1983).
2) F. P. Chen and R. Goulard, JQSRT 16, 819 (1976).
3) R. H. Tourin, Spectroscopic Gas Temperature Measurement. Elsevier, New York (1983).
4) R. Snyder and L. Hesselink, Optic Let. 13, 87 (1988).
5) E. J. Beiting, 28th Aerospace Sciences Meeting, 90-0157, AIAA, Washington, D.C. (1990)
6) Y. R. Sivathanu and J. P. Gore, JQSRT 50, 483 (1993).
7) Y. R. Sivathanu and J. P. Gore, JQSRT 49, 269 (1993).
8) W. H. Dalzell and A. L. Sarofim, J. Heat Trans. 91, 100 (1969).
9) Y. R. Sivathanu, J. P. Gore and J. Dolinar, Combust. Sci. Tech. 76, 45 (1991).
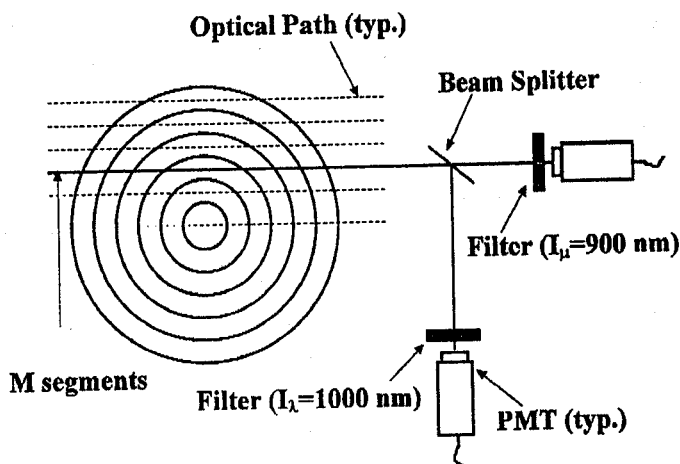
Fig. 1. Experimental arrangement for path integrated measurements
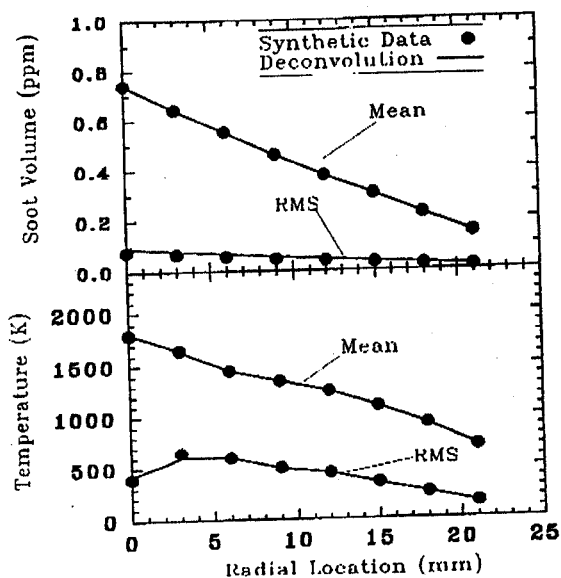
Fig. 2. Radial profiles of the mean and RMS of soot volume fraction and temperature obtained from deconvolution of the synthetic path integrated data
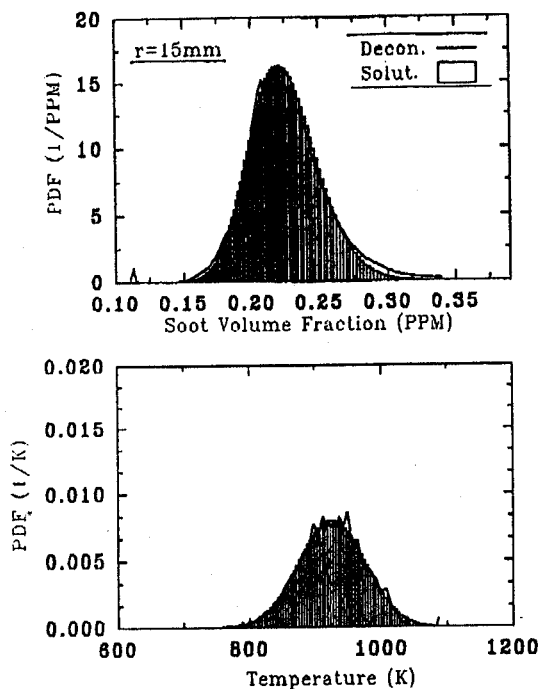
96

Fig. 3. The PDFs of soot volume fraction and temperature obtained from the deconvolution of the synthetic path integrated data.
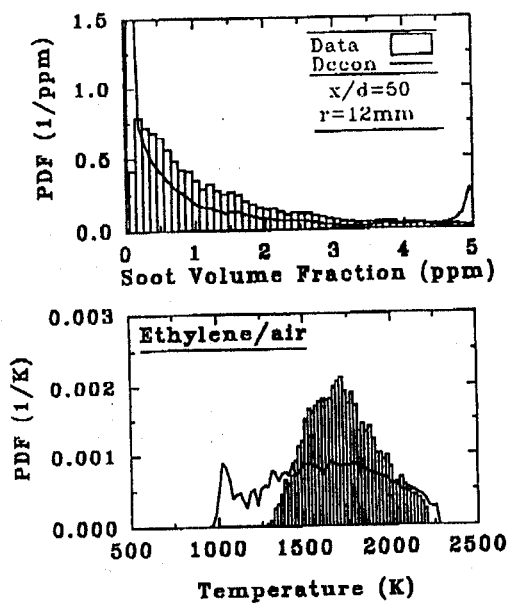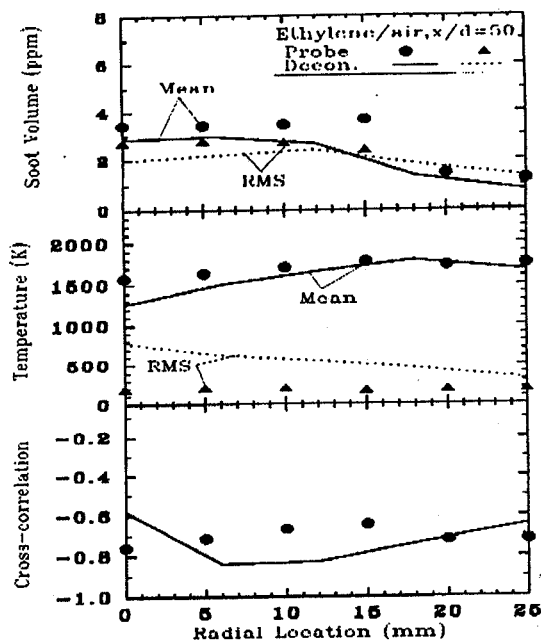

Fig. 4. Radial profiles of the mean and RMS of soot volume fraction and temperature and their cross-correlation in an Ethylene/air diffusion flame.
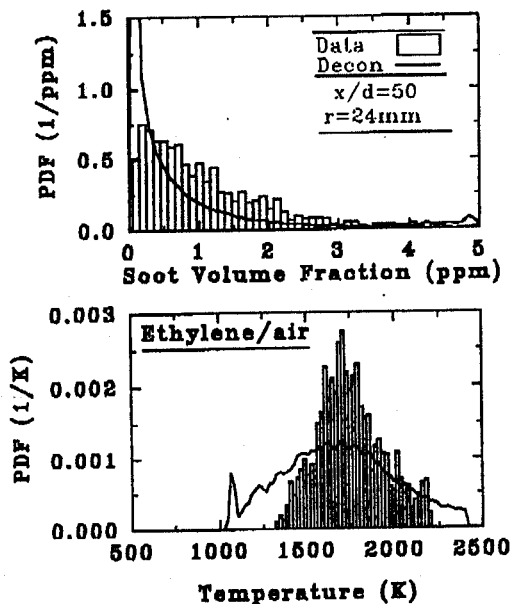

Fig. 5. The PDFs of soot volume fraction and temperature in an Ethylene/air diffusion flame at r=12 mm.

Fig. 6. The PDFs of soot volume fraction and temperature in an Ethylene/air diffusion flame at r=24 mm.